

ChemMedChem

Supporting Information

Albumin Conjugates of Thiosemicarbazone and Imidazole-2-thione Prochelators: Iron Coordination and Antiproliferative Activity

Yu-Shien Sung, Wangbin Wu, Megan A. Ewbank, Rachel D. Utterback, Michael T. Marty, and Elisa Tomat*

Contents

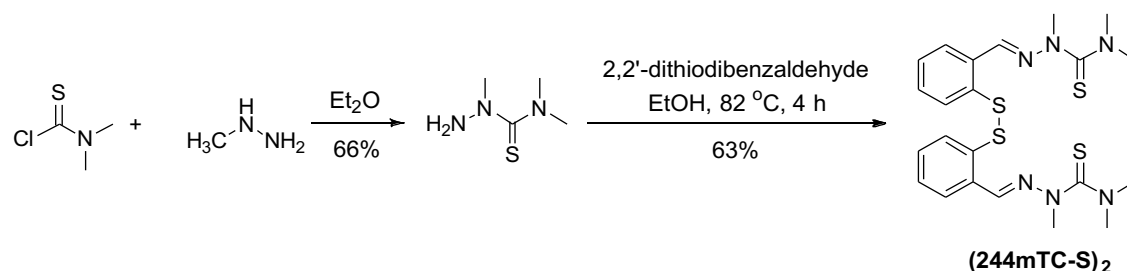
Materials and Methods	S2
Synthetic Procedures (Schemes S1-S3)	S2
Measurement of octanol/water partition coefficients (Table S1)	S5
Formation of complexes in neutral aqueous solutions (Figs. S1-S2)	S6
X-ray diffraction analysis (Table S2, Figs. S3-S4)	S7
Stability of prochelators in aqueous solutions and in the presence of BSA (Figs. S5-S6)	S11
Native mass spectrometry	S12
Cell culture and viability assays	S12
References	S13
NMR spectra (Figs. S7-S18)	S14

Materials and Methods

Disulfide-based prochelators (TC1-S)₂, (TC2-S)₂, (AH1-S)₂ and control thioether TE1 were synthesized as previously reported.^[1, 2] Precursors 2,2'-dithiodibenzaldehyde^[3] and 1-amino-3-methylimidazolium chloride^[4, 5] were synthesized according to reported procedures. Tetrahydrofuran (THF), diethyl ether, *N,N*-dimethylformamide (DMF) and pentane were dried by passage through a solvent purifier. Dry solvents were confirmed to contain < 0.1 ppm H₂O using a Mettler Toledo C10S Coulometric Karl Fisher Titrator. 3-(4,5-dimethylthiazol-2-yl)-2,5-diphenyltetrazolium bromide (MTT) was purchased from VWR and used as received. Deferoxamine mesylate salt (DFO, Sigma-Aldrich) and all other reagents were obtained commercially and used as received.

Chromatographic purifications on silica gel were conducted on a Biotage Isolera One Flash Chromatography Instrument. HPLC analyses were conducted on an Agilent 1260 Infinity II system using a ZORBAZ Eclipse XDB-C18 (9.4 x 250 mm, 5 μm) column. NMR spectra were recorded on a Bruker Advance-III 400 MHz and a Bruker NEO-500 MHz NMR spectrometer at the NMR Spectroscopy Facility of the Department of Chemistry and Biochemistry. The chemical shifts were recorded in ppm relative to tetramethylsilane (SiMe₄, δ = 0 ppm) or with the residual solvent resonance as the internal standard. The continuous-wave EPR measurements were performed at the EPR Facility of the Department of Chemistry and Biochemistry of the University of Arizona, on the Bruker Elexsys E500 continuous-wave EPR spectrometer equipped with a rectangular TE₁₀₂ resonator. Low- and high-resolution mass spectra (LRMS and HRMS) via electrospray ionization (ESI) methods were obtained at the University of Arizona Analytical & Biological Mass Spectrometry Core Facility. Optical absorption spectra were obtained at ambient temperature using an Agilent 8453 UV-Vis spectrophotometer. Elemental analyses were performed by Numega Resonance Labs, San Diego, CA.

Synthetic Procedures

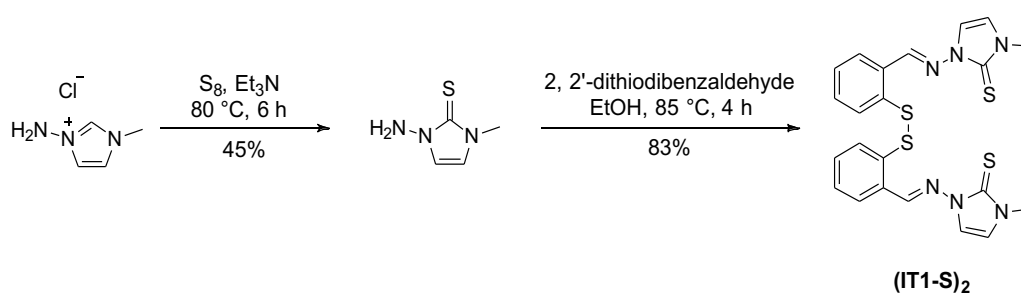


Scheme S1. Synthesis of (244mTC-S)₂.

2,4,4-Trimethylthiosemicarbazide. Thiocarbonyl chloride (1.0 g, 8.1 mmol) and methyl hydrazine (0.85 mL, 16.2 mmol) were dissolved in anhydrous ether at 0 °C. A white precipitate of methylhydrazinium chloride formed and the reaction mixture was allowed to warm up to room temperature and stirred for 16 h. The precipitate was filtered off and the solution was evaporated. The oily residue crystallized at -20 °C, and the crystalline product was collected and washed with cold ether (705 mg, 66%). ¹H NMR (400 MHz, CDCl₃) δ 4.51 (s, 2H), 3.14 (s, 6H), 3.12 (s, 3H). ¹³C

NMR (101 MHz, CDCl₃) δ 195.85, 46.25, 43.21. LRMS-ESI: m/z [M+H]⁺ calcd for C₄H₁₂N₃S⁺, 134.08; found 134.05.

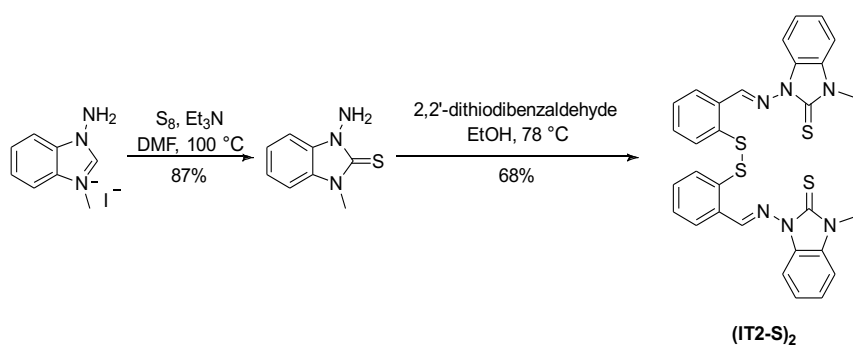
(244mTC-S)₂. Solid 2,4,4-trimethylthiosemicarbazide (0.5 g, 3.6 mmol) and 2, 2'-dithiodibenzaldehyde (0.5 g, 1.8 mmol) were combined and suspended in EtOH (18 mL) and refluxed at 82 °C for 4 h. After evaporation of the solvent, the residue was purified by flash chromatography (95/5 to 70/30, v/v, hexanes/EtOAc) to obtain the product as a white foam (579 mg, 63%). ¹H NMR (400 MHz, CDCl₃) δ 7.83 (dd, J = 7.8, 1.6 Hz, 1H), 7.78 (s, 1H), 7.60 (dd, J = 7.8, 1.4 Hz, 1H), 7.38 - 7.33 (m, 1H), 7.31 - 7.26 (m, 1H), 3.35 (s, 3H), 3.30 (s, 6H). ¹³C NMR (101 MHz, CDCl₃) δ 188.02, 136.84, 135.50, 134.82, 134.54, 129.79, 129.77, 126.18, 44.51, 36.36. HRMS-ESI: m/z [M+H]⁺ calcd for C₂₂H₂₉N₆S₄⁺ 505.1331; found 505.1339; [M+Na]⁺ calcd for C₂₂H₂₈N₆S₄Na⁺ 527.1150; found 527.1154.



Scheme S2. Synthesis of (IT1-S)₂

1-Amino-3-methylimidazole-2-thione. The synthesis followed a reported procedure^[4, 5] with slight modifications. A mixture of 1-amino-3-methylimidazolium chloride (800 mg, 6.0 mmol), S₈ (200 mg, 0.79 mmol), and Et₃N (1.68 mL, 12.0 mmol) in freshly distilled pyridine (8.0 mL) was stirred at 80 °C for 6 h. Pyridine and Et₃N were removed under reduced pressure, and the residue was extracted with EtOAc (10 × 3.0 mL) and dried over anhydrous MgSO₄. The product was purified by flash chromatography (100/0 to 90/10, v/v, CH₂Cl₂/MeOH) and a dark red solid was obtained (349 mg, 45%) ¹H NMR (400 MHz, CDCl₃) δ 6.86 (dd, J = 2.4, 1.1 Hz, 1H), 6.56 (dd, J = 2.4, 1.0 Hz, 1H), 4.88 (s, 2H), 3.58 (d, J = 1.1 Hz, 3H). ¹³C NMR (101 MHz, CDCl₃) δ 162.13, 118.19, 115.28, 35.57. LRMS-ESI: m/z [M+Na]⁺ calcd for C₄H₇N₃SNa⁺ 152.03, found 151.95.

(IT1-S)₂. Solid 1-amino-3-methylimidazole-2-thione (100 mg, 0.77 mmol) and 2,2'-dithiodibenzaldehyde (106 mg, 0.38 mmol) were combined, suspended in ethanol (4.0 mL) and refluxed at 85 °C for 4 h. The product precipitated out from the reaction mixture as a yellow powder and was isolated by filtration without further purification (158 mg, 83%). ¹H NMR (400 MHz, DMSO-*d*₆) δ 9.48 (s, 1H), 7.89 - 7.85 (m, 1H), 7.77 - 7.73 (m, 2H), 7.52 - 7.46 (m, 1H), 7.44 - 7.39 (m, 1H), 7.35 (m, 1H), 3.53 (s, 3H). ¹³C NMR (101 MHz, DMSO-*d*₆) δ 160.71, 152.45, 136.70, 131.67, 131.66, 130.59, 128.54, 127.47, 119.05, 111.86, 34.49. HRMS-ESI m/z : [M+H]⁺ calcd for C₂₂H₂₁N₆S₄⁺, 497.0705, found 497.0697; [M+Na]⁺ calcd for C₂₂H₂₀N₆S₄Na⁺, 519.0524; found 519.0516.



Scheme S3. Synthesis of (IT2-S)₂.

1-Amino-3-methylbenzoimidazole-2-thione. This preparation was modified from a previously reported method.^[6] 1-Amino-3-methyl-1*H*-benzoimidazol-3-ium iodide (514 mg, 2.00 mmol), S₈ (96 mg, 0.38 mmol), and Et₃N (277 μL, 2.00 mmol) were combined in DMF (400 μL). The reaction mixture was heated to 100 °C for 2 h. Upon cooling to room temperature, the solidified reaction mixture was redissolved in CH₂Cl₂ and the desired product was purified via column chromatography (90/10 to 85/15, v/v, hexanes/EtOAc) and recrystallization from MeOH. The desired product (279 mg, 87%) was collected as pale yellow solid. ¹H NMR (400 MHz, CDCl₃) δ 7.41 – 7.37 (m, 1H), 7.28 – 7.19 (m, 2H), 7.16 – 7.11 (m, 1H), 4.85 (s, 2H), 3.72 (s, 3H). ¹³C NMR (101 MHz, CDCl₃) δ 169.56, 132.14, 130.45, 123.36, 123.07, 109.47, 108.81, 31.43. LRMS-ESI *m/z*: [M+H]⁺ calcd for C₈H₁₀N₃S⁺ 180.06; found 179.98.

(IT2-S)₂. 1-Amino-3-methylbenzoimidazole-2-thione (161 mg, 1.00 mmol) and 2,2'-dithiodibenzaldehyde (137 mg, 0.50 mmol) were dissolved in EtOH (10 mL) and stirred at 78 °C for 12 h. Upon cooling of the reaction mixture to room temperature, the desired product was collected as a white powder by filtration, washed with ethanol and dried under vacuum (406 mg, 68%). ¹H NMR (400 MHz, CDCl₃) δ 10.95 (s, 1H), 7.95 – 7.91 (m, 1H), 7.89 – 7.84 (m, 1H), 7.66 – 7.60 (m, 1H), 7.42 – 7.37 (m, 1H), 7.32 – 7.26 (m, 3H), 7.21 – 7.17 (m, 1H), 3.82 (s, 3H). ¹³C NMR (101 MHz, CDCl₃) δ 164.56, 157.20, 138.13, 132.58, 131.82, 131.78, 130.58, 130.37, 129.60, 127.35, 123.95, 123.60, 110.73, 108.64, 30.75. HRMS (ESI-MS) *m/z*: [M+Na]⁺ calcd for C₃₀H₂₄N₆S₄Na⁺ 619.0837; found 619.0844.

Synthesis of thiol-based chelators. In a generally applicable procedure, the disulfide prochelator (1.0 equiv.) and dithiothreitol (DTT, 2.5 equiv.) were combined and dissolved in dry DMF (to a 0.2 M concentration of prochelator). The reaction mixture was stirred at room temperature for 2-4 h under N₂. Addition of degassed, deionized (DI) water caused the formation of a white precipitate, which was collected via centrifugation. The solid was washed with DI water twice to remove residual DTT and the product was then dried under high vacuum and stored under nitrogen to prevent oxidation by air. The yields for this reduction reaction were typically above 90%.

244mTC. ¹H NMR (400 MHz, DMSO-*d*₆) δ 7.88 (s, 1H), 7.69 (m, 1H), 7.43 (m, 1H), 7.20 (m, 2H), 5.80 (brs, 1H), 3.55 (s, 3H), 3.26 (s, 6H). ¹³C NMR (101 MHz, DMSO-*d*₆) δ 187.48, 136.22, 132.05,

131.82, 131.09, 129.02, 128.11, 125.40, 43.87, 36.56. HRMS-ESI m/z : $[M+H]^+$ calcd for $C_{11}H_{16}N_3S_2^+$ 254.0780; found 254.0778; $[M+Na]^+$ calcd for $C_{11}H_{15}N_3S_2Na^+$ 276.0600; found 276.0597.

IT1. 1H NMR (400 MHz, DMSO- d_6) δ 9.21 (s, 1H), 7.87 (d, $J = 2.7$ Hz, 1H), 7.73 (m, 1H), 7.67 (brs, 1H), 7.47 (d, $J = 7.8$ Hz, 1H), 7.39 – 7.34 (m, 2H), 7.29 (t, $J = 7.4$ Hz, 1H), 3.54 (s, 3H). ^{13}C NMR (101 MHz, DMSO- d_6) δ 161.18, 153.38, 135.08, 132.38, 130.79, 130.71, 128.44, 124.93, 119.38, 110.66, 34.51. HRMS-ESI m/z : $[M+H]^+$ calcd for $C_{11}H_{12}N_3S_2^+$ 250.04672; found 250.04671; $[M+Na]^+$ calcd for $C_{11}H_{11}N_3S_2Na^+$, 272.02866; found 272.02861.

Synthesis of Fe complexes

[Fe(244mTC-H)₂][BF₄]. 244mTC (52 mg, 0.2 mmol) was dissolved in dry THF (1 mL) at room temperature under aerobic conditions. Upon addition of $Fe(BF_4)_2 \cdot 6H_2O$ (34.6 mg, 0.1 mmol) to this pale yellow solution, the reaction mixture turned dark brown. The reaction was allowed to stir for 30 min. A dark brown solid was collected and dissolved in acetone (2 mL). Vapor diffusion of *n*-pentane into the acetone solution yielded dark brown crystals within a few days. The light brown acetone/pentane supernatant was transferred out and the crystals were dried under high vacuum. (38.8 mg, 60%) HRMS-ESI m/z $[M]^+$ calcd for $C_{22}H_{28}FeN_6S_4^+$, 560.06025; found 560.06011. Anal. Calcd. ($C_{22}H_{28}FeN_6S_4BF_4$) \cdot 0.5(H_2O): C, 40.3; H, 4.4; N, 12.8. Found: C, 40.3; H, 4.1; N, 12.0.

[Fe(IT1-H)₂][BF₄]. IT1 (30 mg, 0.12 mmol) was dissolved in dry THF (2.5 mL) at room temperature under aerobic conditions. Upon addition of $Fe(BF_4)_2 \cdot 6H_2O$ (20.3 mg, 0.06 mmol), the pale yellow solution turned dark brown. The reaction was allowed to stir for 30 min, and the precipitation of a dark brown solid was observed. The solid was collected by filtration and dissolved in acetone (1.5 mL). Vapor diffusion of *n*-pentane into the acetone solution yielded dark brown crystals within a few days. The light brown acetone/pentane supernatant was removed and the crystals were dried under high vacuum. (16.7 mg, 40%) HRMS-ESI m/z $[M]^+$ calcd for $C_{22}H_{20}FeN_6S_4^+$, 551.99765; found 551.99703. Anal. Calcd. ($C_{22}H_{20}FeN_6S_4BF_4$) \cdot (CH_3COCH_3): C, 43.1; H, 3.8; N, 12.0. Found: C, 43.3; H, 3.1; N, 12.0.

Measurement of octanol/water partition coefficients (log P values)

The log P values for the disulfide prochelators were obtained using the stir-flask method and analytical HPLC to determine relative concentrations of the compounds in the two phases.^[7] Octanol was pre-saturated with nano-pure water by stirring vigorously for 18 h at room temperature. A solution containing the disulfide compound (1.0 mM) in octanol (2.0 mL) was added to a vial containing nano-pure water (2.0 mL). The tube was stirred vigorously at room temperature for 12 h. The two phases were allowed to separate for 3 h and transferred to separate tubes. The solutions were centrifuged for 10 min at 6400 rpm to remove any turbidity due to small immiscible droplets. The *n*-octanol phase solution was diluted 100 times prior to HPLC analysis. The log P value were calculated according to the following formula:

$$\text{Log } P_{ow} = \text{Log} \left(\frac{c_{n-octanol}}{c_{water}} \right) = \text{Log} \left(\frac{100 * A_{n-octanol}}{A_{water}} \right)$$

where c refers to compound concentrations and A refers to chromatographic peak area. All experiments were carried out in triplicate (Table S1).

Table S1. Octanol/water log P values of prochelators

Compound	Data			Log P
(244mTC-S) ₂	4.03	4.05	3.91	4.0 ± 0.1
(IT1-S) ₂	3.13	3.24	3.53	3.3 ± 0.2
(IT2-S) ₂	n.d.	n.d.	n.d.	(6.57) ^[a]
(TC2-S) ₂	2.08	1.78	2.20	2.0 ± 0.2
Dp44mT	1.84	1.90	2.30	2.0 ± 0.2

[a] Predicted consensus log P value obtained via the Swiss ADME web tool.^[8]

Formation of complexes in neutral aqueous conditions

C₂₂H₂₈FeN₆S₄ corr #17-34 RT: 0.13-0.21 AV: 18 NL: 4.99E8
T: FTMS + p ESI Full ms [130.0000-1000.0000]

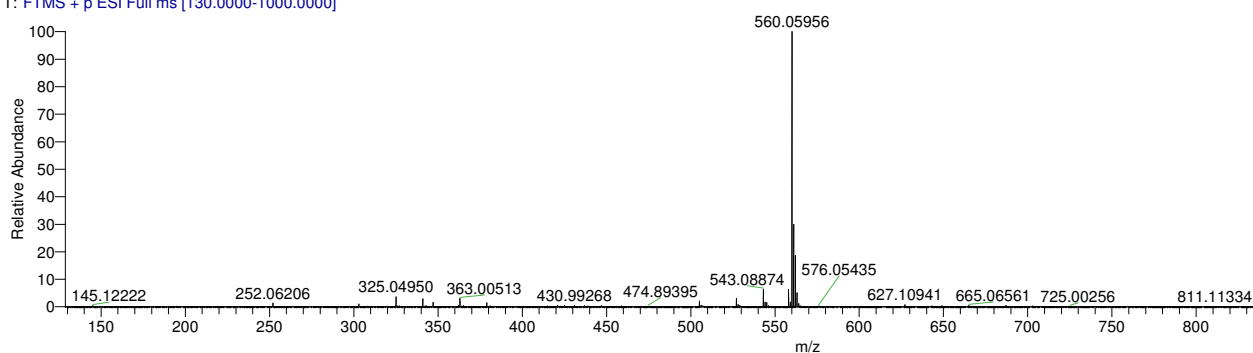


Figure S1. ESI mass spectrum of $[\text{Fe}(\text{244mTC-H})_2]^+$ (calculated m/z $[\text{C}_{22}\text{H}_{28}\text{FeN}_6\text{S}_4]^+$ 560.06025) obtained upon addition of Fe(II) (0.5 equiv) to thiol chelator 244mTC in a buffered aqueous solution (50 mM PIPES, 100 mM KCl, pH 7.4). The aqueous solution was degassed with N₂ for 30 min prior to addition of the reactants; however, the reaction was conducted under aerobic conditions and a color change from pale yellow to brown was observed instantly.

C22H20FeN6S4 #17-25 RT: 0.13-0.18 AV: 9 NL: 1.35E7
T: FTMS + p ESI Full ms [130.0000-1000.0000]

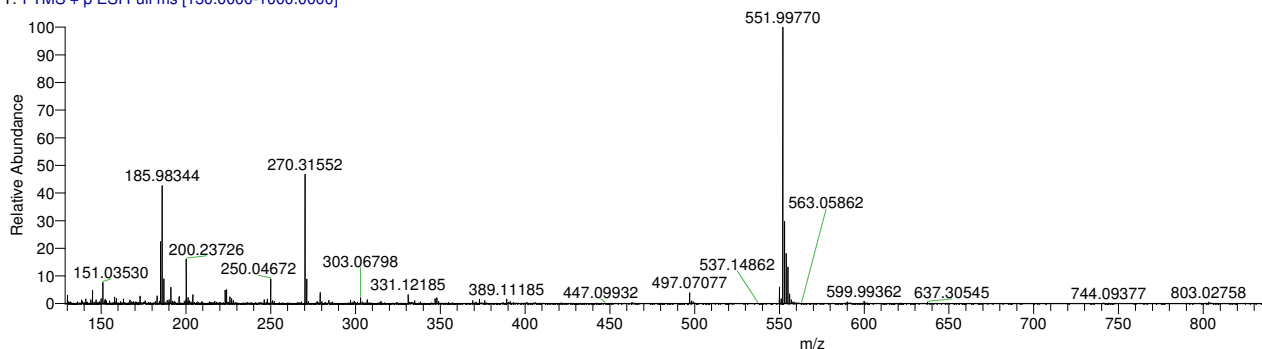


Figure S2. ESI mass spectrum of $[\text{Fe}(\text{IT1-H})_2]^+$ (calculated m/z $[\text{C}_{22}\text{H}_{20}\text{FeN}_6\text{S}_4]^+$ 551.99765) obtained upon addition of Fe(II) (0.5 equiv) to thiol chelator IT1 in a buffered aqueous solution (50 mM PIPES, 100 mM KCl, pH 7.4). The aqueous solution was degassed with N_2 for 30 min prior to addition of the reactants; however, the reaction was conducted under aerobic conditions and a color change from pale yellow to brown was observed instantly.

X-Ray diffraction analysis

The single-crystal XRD measurements were performed at the XRD Facility of the Department of Chemistry and Biochemistry of the University of Arizona, using a Bruker Kappa APEX II DUO diffractometer equipped with molybdenum and copper X-ray sources, APEX II CCD area detector, four-circle kappa goniometer, and an Oxford Cryostream nitrogen-flow system. The diffraction data were collected at the temperature of 100 K, under the $\text{Mo-K}\alpha$ radiation ($\lambda = 0.71073 \text{ \AA}$). The diffractometer was controlled by the APEX2 software package (Bruker AXS Inc., Madison, WI, 2007). The collected diffraction data were corrected for absorption effects using a multi-scan method in SADABS (Sheldrick, G. M. University of Göttingen, Germany, 1997). The structure was solved with the ShelXT^[9] program using Intrinsic Phasing and refined with the ShelXL^[10] package using Least Squares minimization. These programs were called from the Olex2^[11] graphic environment, which also provided for a convenient structure manipulation. The details of structure refinement are shown in Table S2.

Structure refinement of $[\text{Fe}(\text{244mTC-H})_2][\text{BF}_4]$. Crystals grew as dark brown rectangular plates by slow vapor diffusion of pentane into acetone at room temperature. Data were solved and refined in the monoclinic space group $\text{P}2_1/\text{c}$. There were 8 complexes per unit cell, 2 complexes per asymmetric unit. The asymmetric unit contained two complexes and two $[\text{BF}_4]^-$ counterions. In addition, there were two highly disordered acetone molecules, which were masked out during the refinement using the solvent mask as implemented in Olex2. The excluded regions contained 62 electrons, which corresponded to 2 acetone molecules (32 electrons per molecule). All wholly occupied non-H atoms were located in the Fourier map and refined anisotropically. Carbon-bound hydrogen atoms were placed in ideal calculated positions, with isotropic displacement parameters

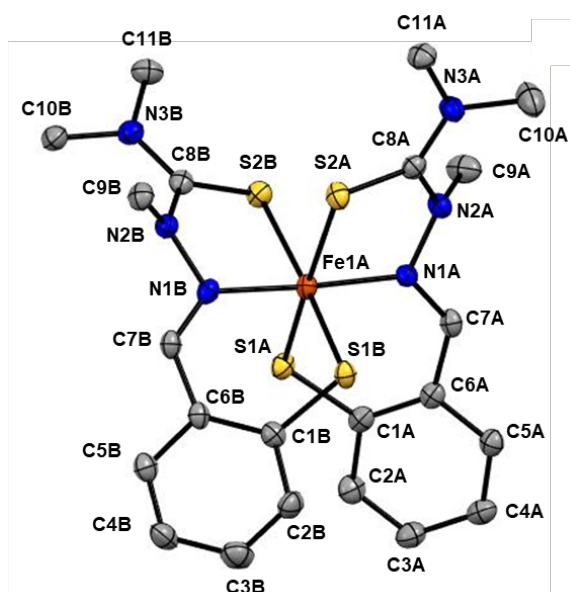
set to $1.2U_{eq}$ of the host carbon atom ($1.5U_{eq}$ for methyl hydrogen atoms). Their positions were then refined using a riding model. The highest residual Fourier peak found in the model was $0.97 \text{ e } \text{\AA}^{-3}$ approx. 1.20 \AA from F1A, and the deepest Fourier hole was $-0.59 \text{ e } \text{\AA}^{-3}$ approx. 0.43 \AA from F1A.

Structure refinement of $[\text{Fe}(\text{IT1-H})_2][\text{BF}_4]$. Crystals grew as dark brown rectangular plates by slow vapor diffusion of pentane into acetone at room temperature. Data were solved and refined in the monoclinic space group $P2_1/n$. There were 4 molecules per unit cell, with one molecule per asymmetric unit. Each iron complex and $[\text{BF}_4]^-$ counterion cocrystallized with two acetone molecules. All wholly occupied non-H atoms were located in the Fourier map and refined anisotropically. Carbon-bound hydrogen atoms were placed in ideal calculated positions, with isotropic displacement parameters set to $1.2U_{eq}$ of the host carbon atom ($1.5U_{eq}$ for methyl hydrogen atoms). Their positions were then refined using a riding model. The highest residual Fourier peak found in the model was $0.41 \text{ e } \text{\AA}^{-3}$ approx. 1.10 \AA from F1, and the deepest Fourier hole was $-0.23 \text{ e } \text{\AA}^{-3}$ approx. 0.25 \AA from H11D.

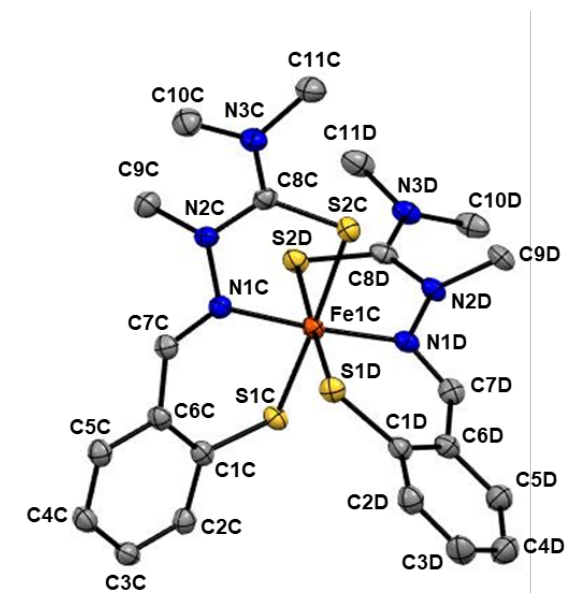
Table S2. Crystallographic information for [Fe(244mTC-*H*)₂][BF₄] and [Fe(IT1-*H*)₂][BF₄]

Complex	[Fe(244mTC- <i>H</i>) ₂][BF ₄]	[Fe(IT1- <i>H</i>) ₂][BF ₄]
Empirical formula	[C ₂₂ H ₂₈ FeN ₆ S ₄][BF ₄]	[C ₂₂ H ₂₀ FeN ₆ S ₄][BF ₄]•2(C ₃ H ₆ O)
Formula weight/g•mol⁻¹	647.40	755.49
Temperature/K	100.0	100.0
Crystal system	monoclinic	monoclinic
Space group	P2 ₁ /c	P2 ₁ /n
a/Å	10.2225(5)	8.2261(4)
b/Å	31.6084(15)	20.4857(11)
c/Å	19.9575(10)	19.8120(11)
α/°	90	90
β/°	99.990(2)	91.812(2)
γ/°	90	90
Volume/Å³	6350.8(5)	3337.0(3)
Z	8	4
ρ_{calc}/cm³	1.354	1.504
μ/mm⁻¹	0.783	0.762
F(000)	2664.0	1556.0
Crystal size/mm³	0.42 × 0.2 × 0.04	0.55 × 0.19 × 0.12
Radiation	MoKα (λ = 0.71073)	MoKα (λ = 0.71073)
2θ range for data collection/°	2.576 to 52.654	2.86 to 52.688
Index ranges	-12 ≤ h ≤ 12, -39 ≤ k ≤ 39, -24 ≤ l ≤ 24	-10 ≤ h ≤ 10, -25 ≤ k ≤ 25, -24 ≤ l ≤ 18
Reflections collected	66717	33571
Independent reflections	12898 [R _{int} = 0.0666, R _{sigma} = 0.0497]	6808 [R _{int} = 0.0287, R _{sigma} = 0.0216]
Data/restraints/parameters	12898/1/697	6808/0/421
Goodness-of-fit on F²	0.968	1.045
Final R indexes [I ≥ 2σ (I)]	R ₁ ^a = 0.0456, wR ₂ ^b = 0.1319	R ₁ ^a = 0.0294, wR ₂ ^b = 0.0725
Final R indexes [all data]	R ₁ = 0.0651, wR ₂ = 0.1462	R ₁ = 0.0345, wR ₂ = 0.0759
Largest diff. peak/hole / e Å⁻³	0.97/-0.59	0.41/-0.23
CCDC	2060902	2060901

$$^a R_1 = \sum [|F_o| - |F_c|] / \sum |F_o|; \quad ^b wR_2 = [\sum w(F_o^2 - F_c^2) / \sum wF_o^4]^{1/2}$$



Bond	Length/Å	Bond	Length/Å
Fe1A-S1A	2.2206(9)	N3A-C8A	1.328(4)
Fe1A-S1B	2.2312(9)	N3A-C11A	1.478(4)
Fe1A-S2B	2.3583(9)	N3A-C10A	1.476(4)
Fe1A-S2A	2.3500(9)	F4A-B1A	1.372(5)
Fe1A-N1A	1.934(2)	C6B-C7B	1.448(4)
Fe1A-N1B	1.932(3)	C6B-C5B	1.419(4)
S1A-C1A	1.753(3)	C6B-C1B	1.414(4)
S1B-C1B	1.746(3)	F3A-B1A	1.338(6)
S2B-C8B	1.701(3)	F2A-B1A	1.423(6)
S2A-C8A	1.706(3)	C7A-C6A	1.452(4)
N1A-N2A	1.435(3)	F1A-B1A	1.378(5)
N1A-C7A	1.290(4)	C1A-C6A	1.414(4)
N2A-C8A	1.378(4)	C1A-C2A	1.407(4)
N2A-C9A	1.472(4)	C6A-C5A	1.411(4)
N2B-N1B	1.426(3)	C3A-C2A	1.388(5)
N2B-C8B	1.370(4)	C3A-C4A	1.406(5)
N2B-C9B	1.481(4)	C5A-C4A	1.384(4)
N1B-C7B	1.303(4)	C5B-C4B	1.373(5)
N3B-C8B	1.342(4)	C1B-C2B	1.404(4)
N3B-C10B	1.467(4)	C2B-C3B	1.390(5)
N3B-C11B	1.465(4)	C4B-C3B	1.393(5)



Bond	Length/Å	Bond	Length/Å
Fe1C-S1C	2.2326(9)	N3D-C10D	1.462(4)
Fe1C-S1D	2.2141(9)	N3D-C11D	1.457(4)
Fe1C-S2C	2.3319(9)	F4A-B1A	1.372(5)
Fe1C-S2D	2.3341(9)	F3C-B1C	1.379(5)
Fe1C-N1D	1.920(3)	N3C-C8C	1.333(4)
Fe1C-N1C	1.934(3)	N3C-C10C	1.466(4)
S1C-C1C	1.749(3)	N3C-C11C	1.465(4)
S1D-C1D	1.742(3)	C7D-C6D	1.439(4)
S2C-C8C	1.699(3)	C7C-C6C	1.451(4)
S2D-C8D	1.705(3)	C2C-C3C	1.382(5)
F4C-B1C	1.379(5)	C2C-C1C	1.415(4)
F1C-B1C	1.364(5)	C5C-C6C	1.428(4)
N1D-N2D	1.430(3)	C5C-C4C	1.377(5)
N1D-C7D	1.304(4)	C1D-C6D	1.429(4)
N1C-N2C	1.437(4)	C1D-C2D	1.408(5)
N1C-C7C	1.303(4)	C6C-C1C	1.412(4)
N2D-C9D	1.480(4)	C6D-C5D	1.419(5)
N2D-C8D	1.362(4)	C3C-C4C	1.402(5)
N2C-C8C	1.383(4)	F2C-B1C	1.341(5)
N2C-C9C	1.484(4)	C2D-C3D	1.371(5)
N3D-C8D	1.340(4)	C5D-C4D	1.385(5)
N3D-C10D	1.462(4)	C4D-C3D	1.402(5)

Figure S3. Structures of the two complexes in the asymmetric unit of $[\text{Fe}(244\text{mTC-H})_2][\text{BF}_4]$ showing the full labeling scheme. The hydrogen atoms in calculated positions and the tetrafluoroborate counterions are not shown. All bond lengths are shown in the tables.

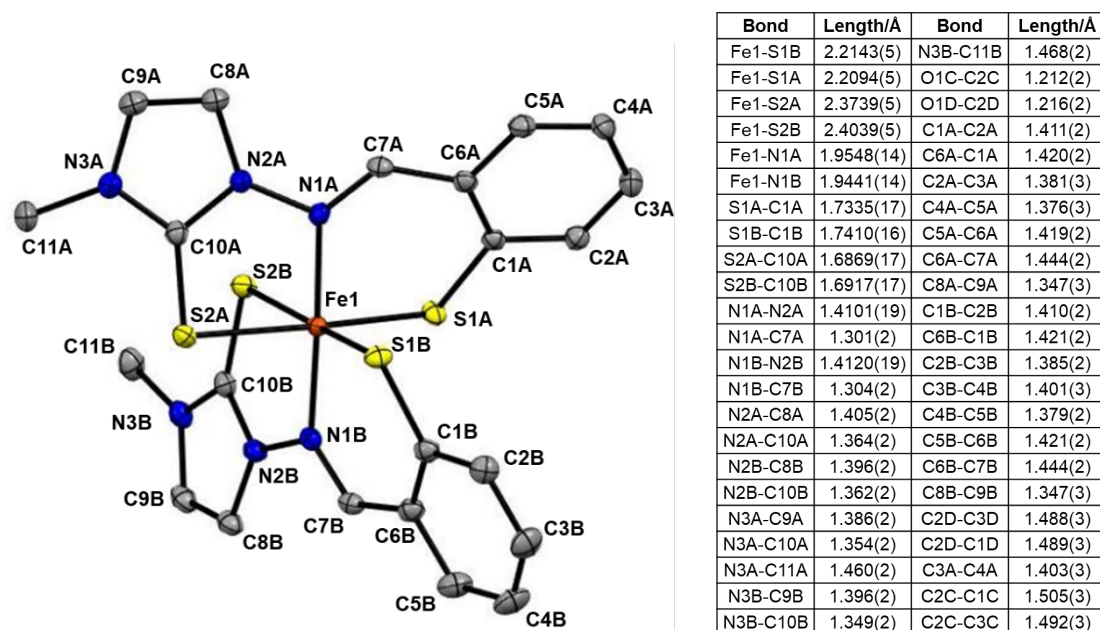


Figure S4. Crystal structure of [Fe(IT1-H)₂][BF₄] showing the full labeling scheme and table of all bond lengths. The hydrogen atoms in calculated positions, the tetrafluoroborate counterion, and two acetone molecules are not shown.

Stability of prochelators in aqueous solutions and in the presence of BSA

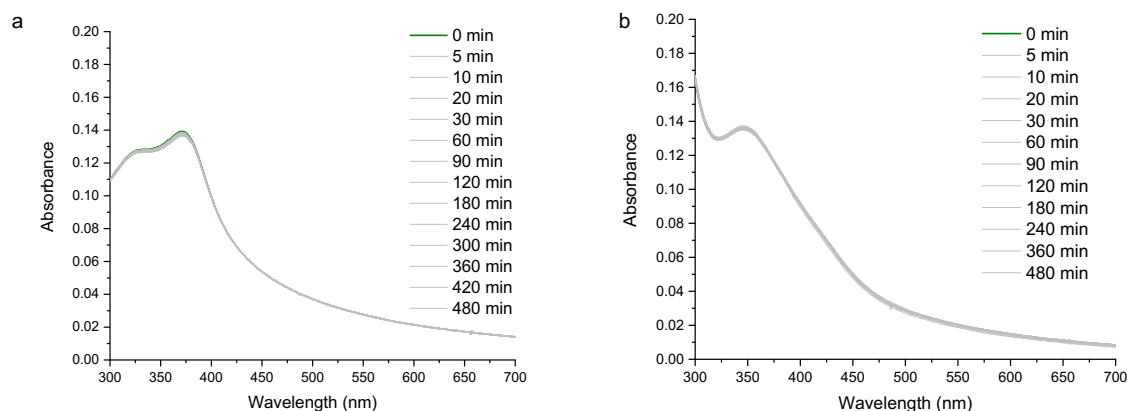


Figure S5. Optical absorption spectra of the prochelators in PBS solutions (pH 7.40) at room temperature over a period of 8 h: a) (244mTC-S)₂, 5 μM, 0.05% DMSO in PBS; b) (IT1-S)₂, 10 μM, 0.1% DMSO in PBS.

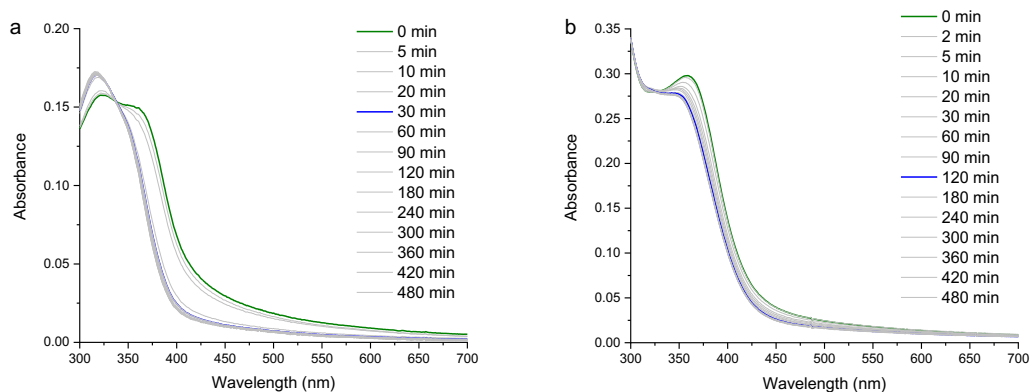


Figure S6. Optical absorption spectra of the prochelators in PBS solutions (pH 7.40) in the presence of BSA (40 μ M) at room temperature over a period of 8 h: a) (244mTC-S)₂, 5 μ M, 0.05% DMSO in PBS; b) (IT1-S)₂, 15 μ M, 0.15% DMSO in PBS.

Native mass spectrometry

Native mass spectra were recorded on a Q-Exactive HF Orbitrap with Ultra High Mass Range modifications (Thermo Fisher Scientific) using previously described methods.^[12] The mass spectrometer was operated with spray voltages of 1.1–1.3 kV, and collisional activation was applied using HCD voltages of 100–150 V. Data were deconvolved and analyzed using UniDec.^[13]

BSA (Sigma Aldrich) samples for native mass spectrometry were solubilized in 0.2 M ammonium acetate (pH 6.8), then buffer-exchanged into fresh 0.2 M ammonium acetate (pH 6.8) twice using Micro Bio-Spin 6 columns (BioRad). The BSA solutions (1 μ M) were incubated with each compound (10 μ M) for 24 h at room temperature.

Cell culture and viability assays

The A2780 (Fox Chase Cancer Center, 03-26) and HT-29 (ATCC[®] HTB-38[™]) cells were grown in RPMI medium (Corning[®] RPMI 1640) supplemented with 10% fetal bovine serum and 1% penicillin/streptomycin. MDA-MB-231 (ATCC[®] HTB-26[™]), MCF-7 (ATCC[®] HTB-22[™]), Caco-2 (ATCC[®] HTB-37[™]) MRC-5 (ATCC[®] CCL-171[™]) cell lines were maintained in Eagle's Minimum Essential Medium (Corning[®] 500 mL MEM) supplemented with 10% fetal bovine serum, penicillin (100 I.U./mL) and streptomycin (100 μ g/mL). All cells were cultured at 37 °C in a humidified atmosphere containing 5% CO₂.

MTT (3-(4,5-dimethylthiazol-2-yl)-2,5-diphenyltetrazolium bromide) viability assays were conducted by standard methods with slight modifications. Cells were seeded with the following cell density per well in 96-well plates: A2780, 2000 cells/well; MDA-MB-231, 2000 cells/well; MCF-7, 3000 cells/well; Caco-2, 3500 cells/well; HT-29, 3500 cells/well; MRC-5, 5000 cells/well, and allowed to attach for 24 h. Test compounds dissolved in DMSO were diluted in growth medium to the specified concentration (with final DMSO concentration limited to 0.1%). Cells were incubated in the presence of the test compounds (200 μ L in medium) for 72 h. After removal of the media containing the test compounds, the MTT solution (prepared in medium without FBS, 0.5 mg/mL) was added to each

well (100 μ L) and incubated for 4 h. Following media removal, DMSO (200 μ L) was added to each well to dissolve the purple formazan crystals and the plates were incubated at 37 °C for 30 minutes. Absorption at 570 nm was recorded on a BioTek Synergy™ 2 microplate reader and data were analyzed using logarithmic fits to obtain IC₅₀ values. The reported IC₅₀ values are the average of at least three independent experiments, and values are given as mean plus/minus standard deviation.

References

- [1] E. A. Akam, R. D. Utterback, J. R. Marcero, H. A. Dailey, E. Tomat, *J. Inorg. Biochem.* **2018**, *180*, 186-193.
- [2] T. M. Chang, E. Tomat, *Dalton Trans.* **2013**, *42*, 7846-7849.
- [3] H. S. Kasmai, S. G. Mischke, *Synthesis* **1989**, *1989*, 763-765.
- [4] G. Laus, V. Kahlenberg, K. Wurst, T. Müller, H. Kopacka, H. Schottenberger, *Z. Naturforsch. B* **2013**, *68*, 1239-1252.
- [5] C. Legault, A. B. Charette, *J. Org. Chem.* **2003**, *68*, 7119-7122.
- [6] T. A. Kuz'menko, V. V. Kuz'menko, A. F. Pozharskii, O. V. Kryshtalyuk, G. G. Aleksandrov, *Chem. Heterocycl. Compd.* **1992**, *28*, 167-176.
- [7] D. N. Brooke, A. J. Dobbs, N. Williams, *Ecotox. Environ. Safe.* **1986**, *11*, 251-260.
- [8] A. Daina, O. Michielin, V. Zoete, *Sci. Rep.* **2017**, *7*, 42717.
- [9] G. Sheldrick, *Acta Cryst.* **2015**, *A71*, 3-8.
- [10] G. Sheldrick, *Acta Cryst.* **2015**, *C71*, 3-8.
- [11] O. V. Dolomanov, L. J. Bourhis, R. J. Gildea, J. A. K. Howard, H. Puschmann, *J. Appl. Cryst.* **2009**, *42*, 339-341.
- [12] J. A. Townsend, J. E. Keener, Z. M. Miller, J. S. Prell, M. T. Marty, *Anal. Chem.* **2019**, *91*, 14765-14772.
- [13] M. T. Marty, A. J. Baldwin, E. G. Marklund, G. K. A. Hochberg, J. L. P. Benesch, C. V. Robinson, *Anal. Chem.* **2015**, *87*, 4370-4376.

NMR Spectra (^1H and ^{13}C)

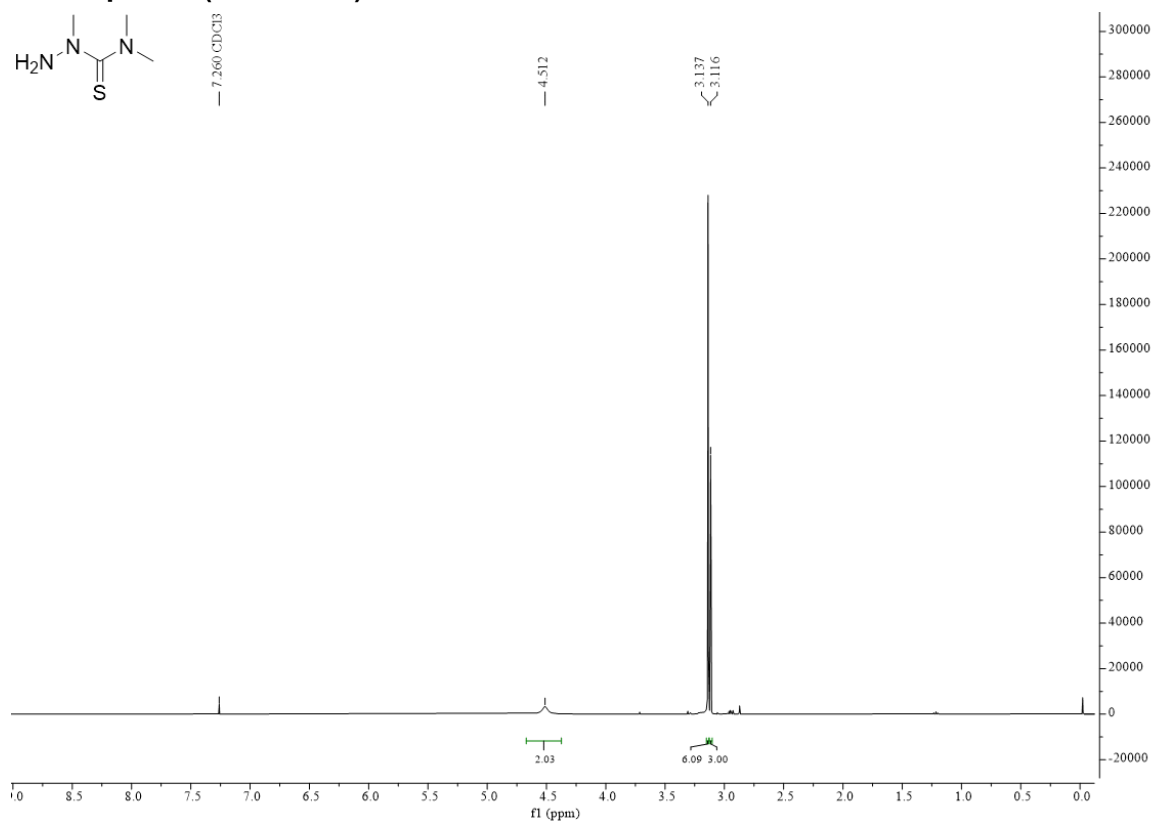


Figure S7. ^1H NMR spectrum of 2,4,4-trimethylthiosemicarbazide (400 MHz, CDCl_3).

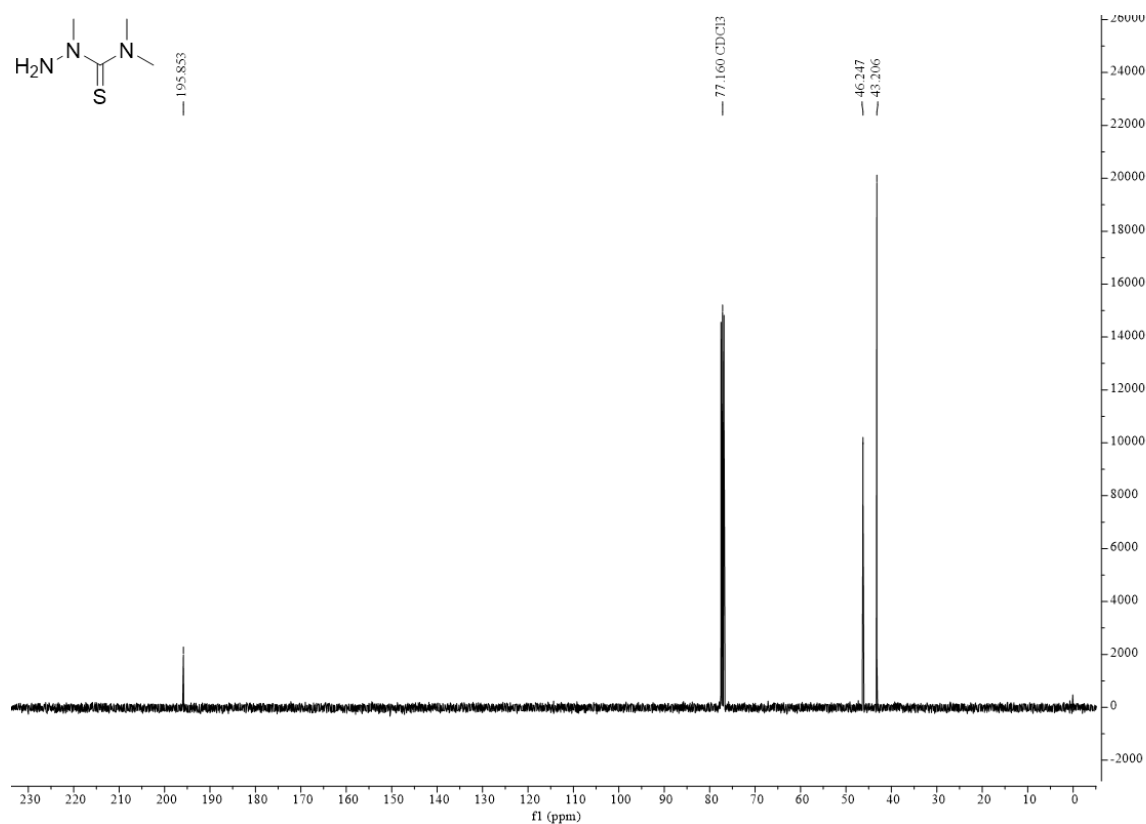


Figure S8. ^{13}C NMR spectrum of 2,4,4-trimethylthiosemicarbazide (101 MHz, CDCl_3).

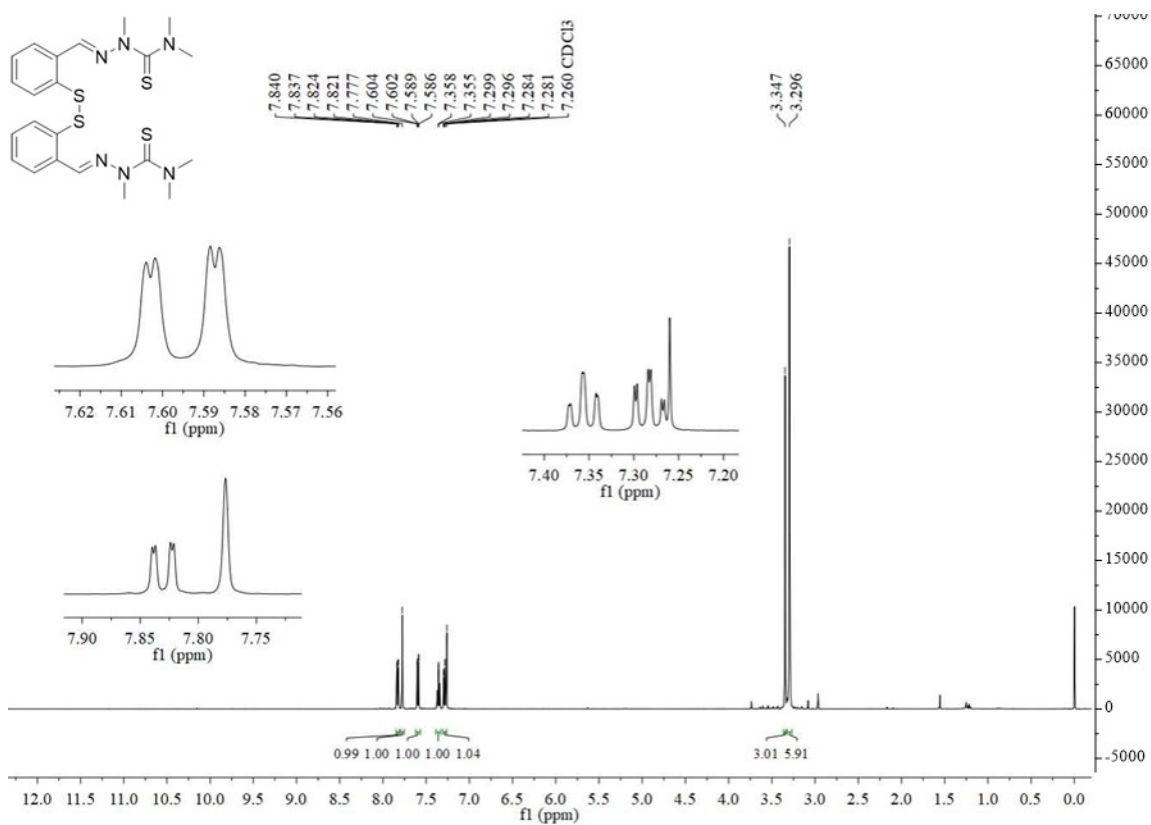


Figure S9. 1H NMR spectrum of $(244mTC-S)_2$ (400 MHz, $CDCl_3$).

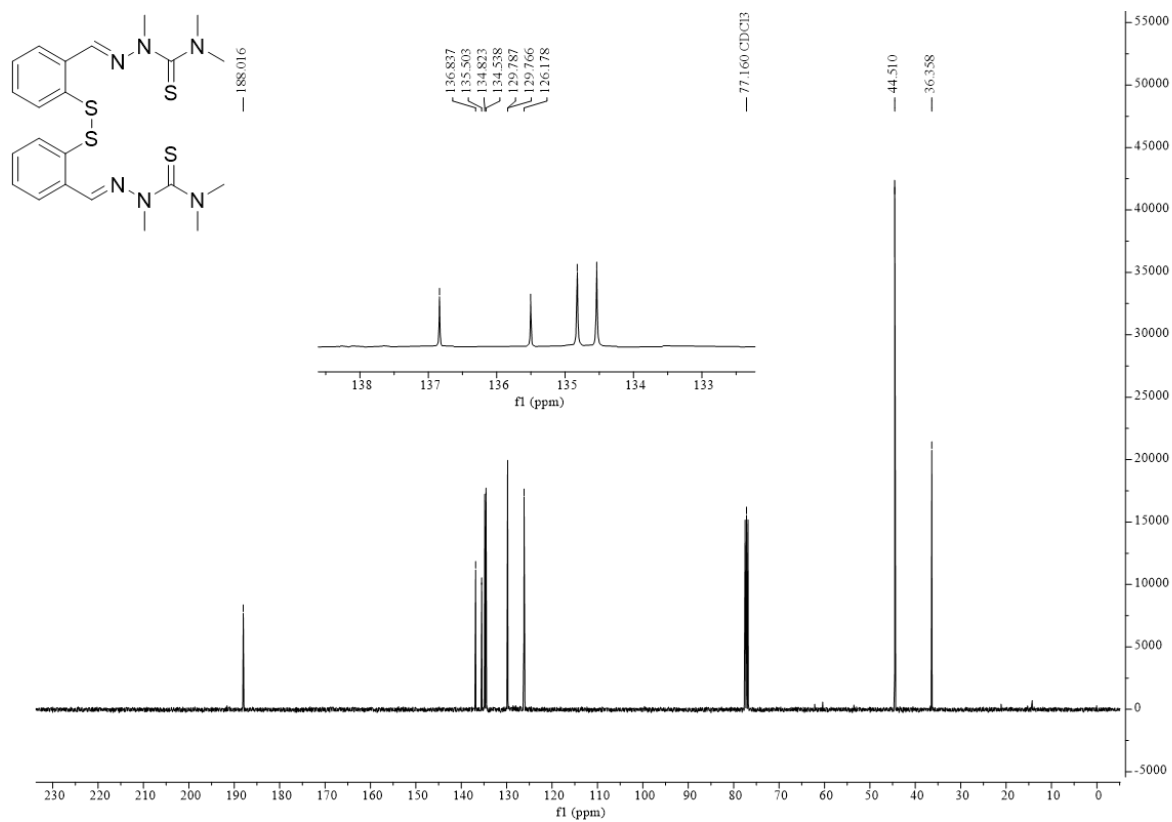


Figure S10. ^{13}C NMR spectrum of $(244mTC-S)_2$ (101 MHz, $CDCl_3$).

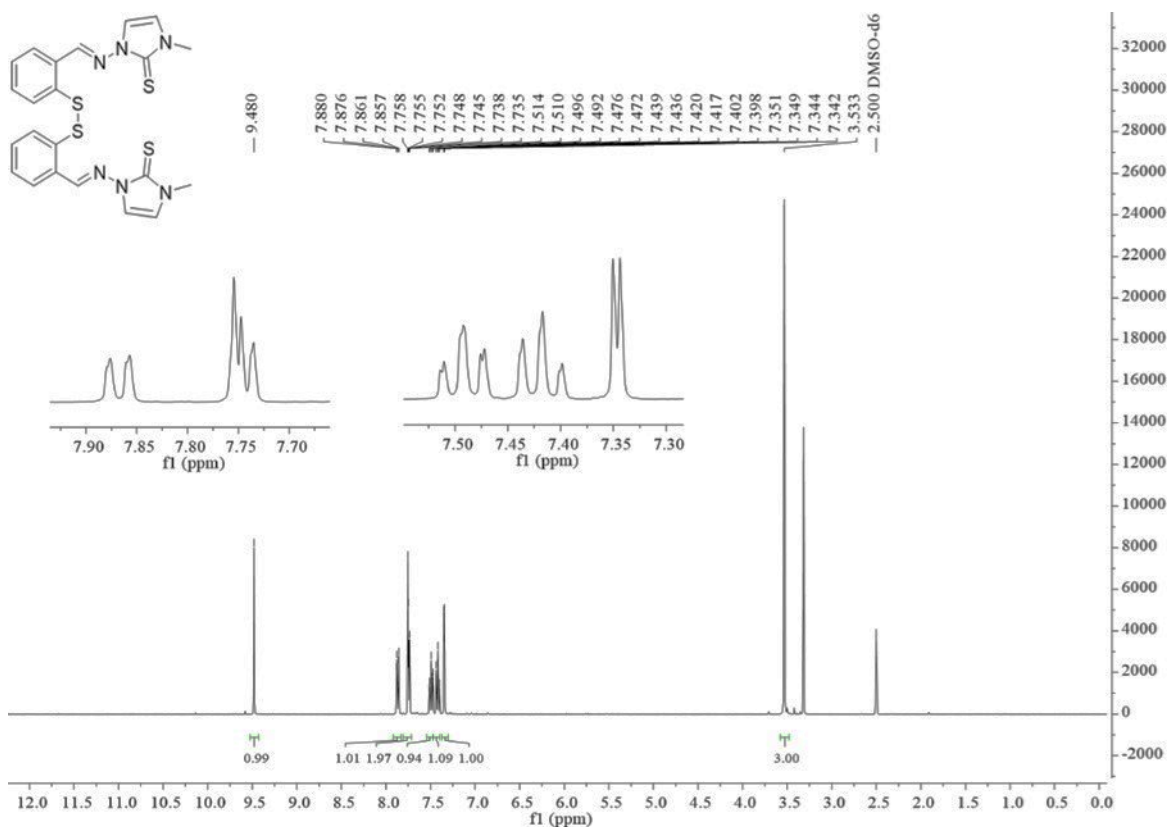


Figure S11. 1H NMR spectrum of $(IT1-S)_2$ (400 MHz, $DMSO-d_6$).

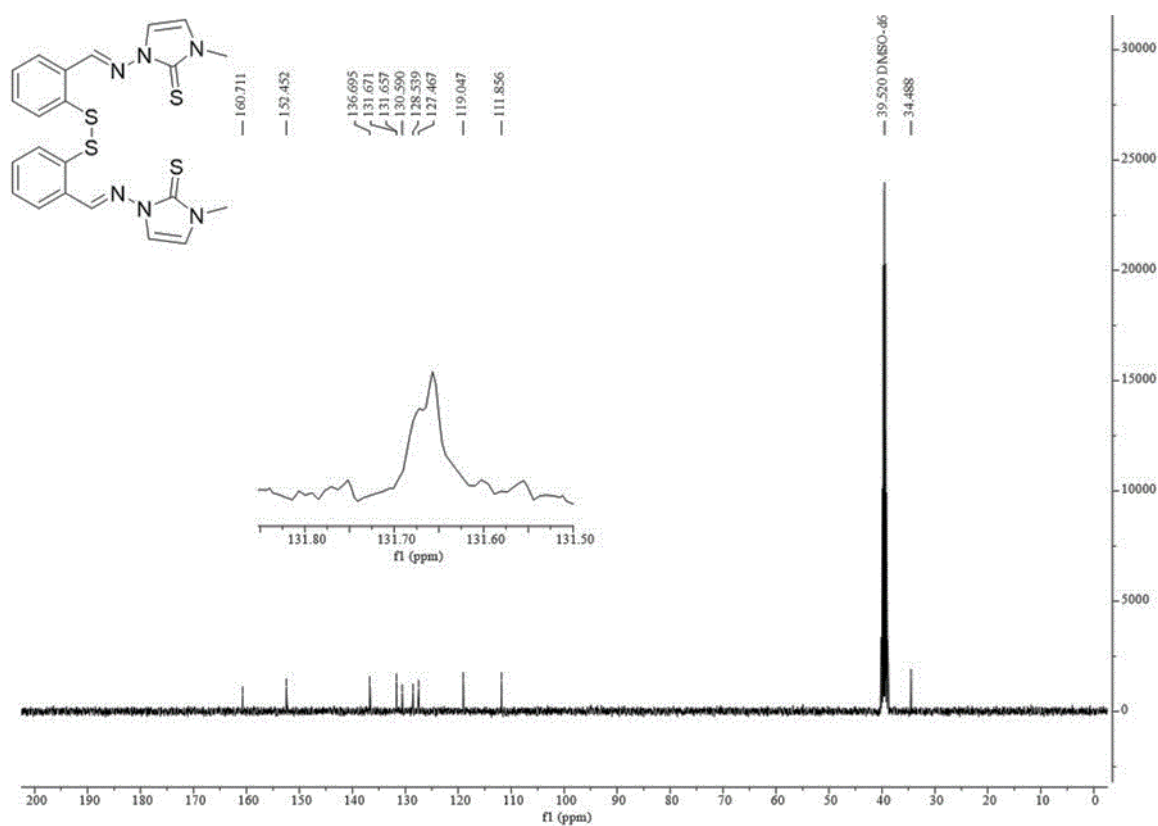


Figure S12. ^{13}C NMR spectrum of $(IT1-S)_2$ (101 MHz, $DMSO-d_6$).

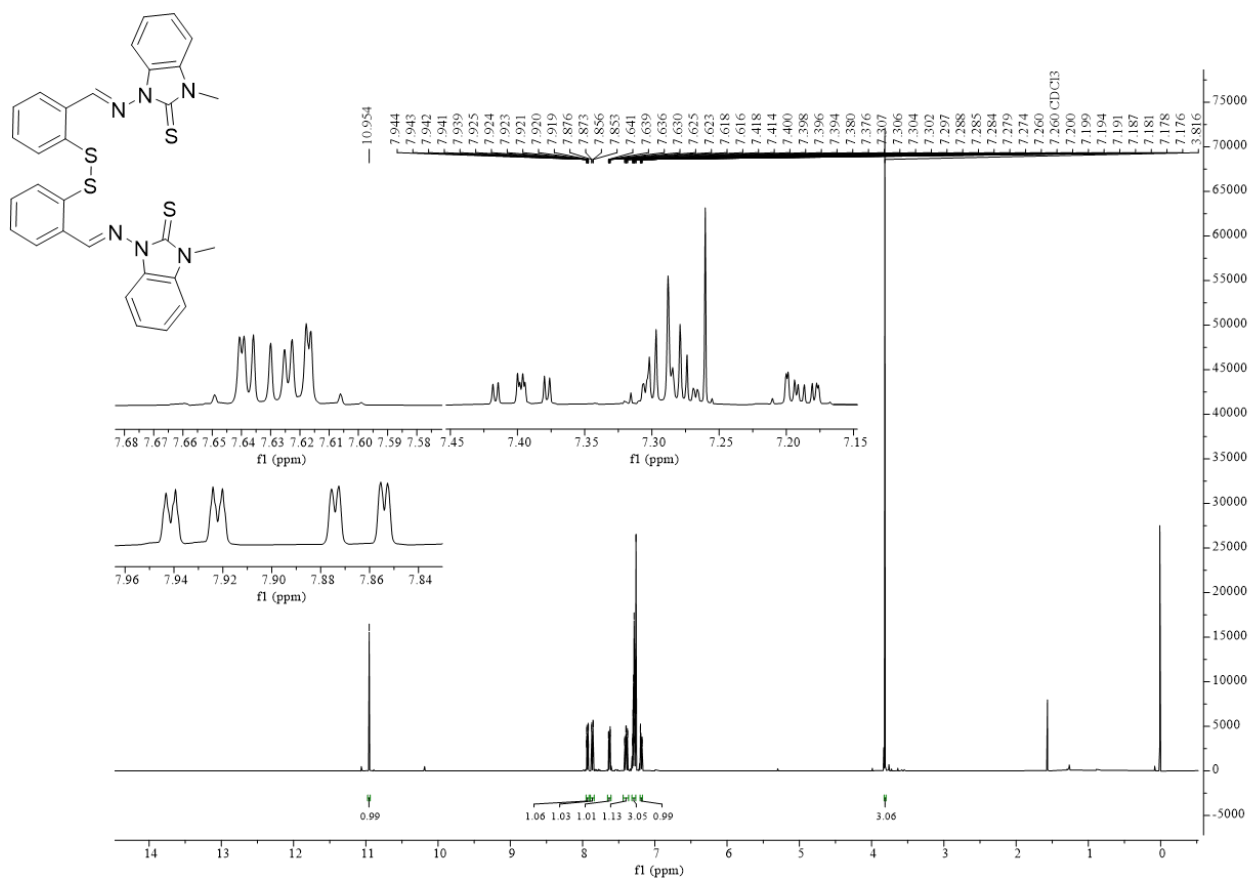


Figure S13. 1H NMR spectrum of $(IT2-S)_2$ (400 MHz, $CDCl_3$).

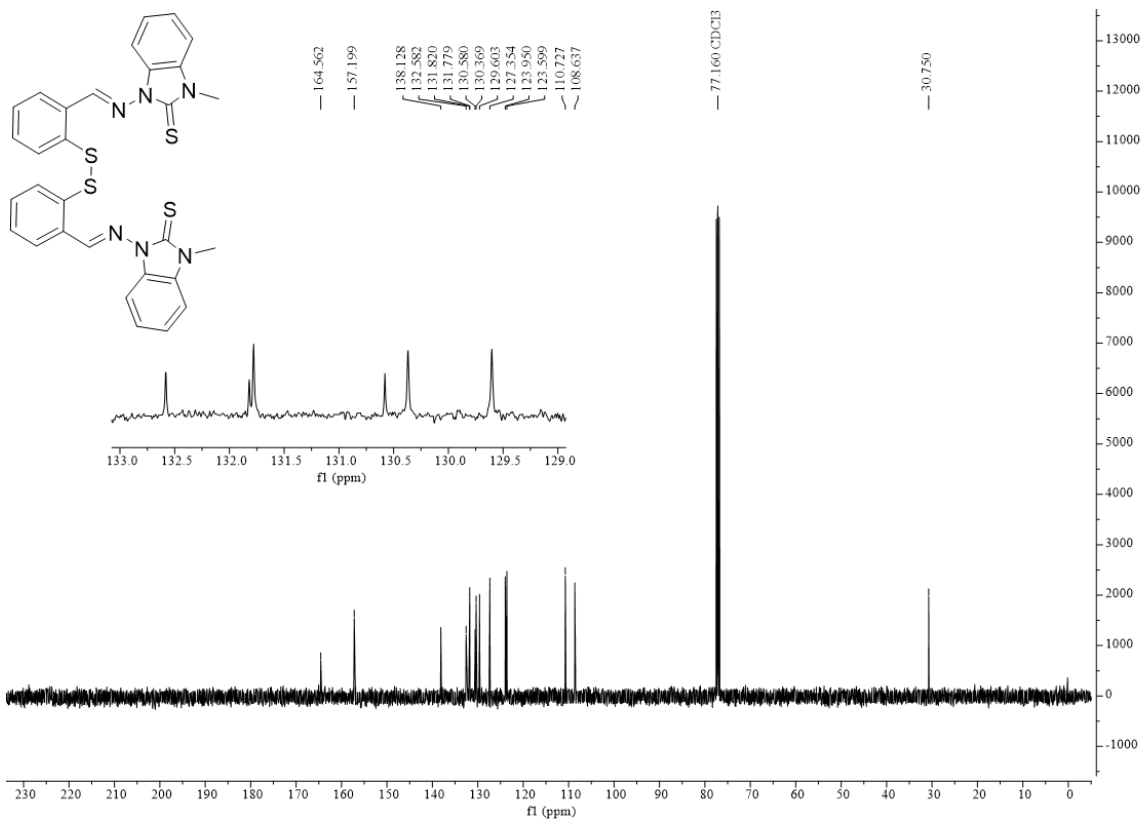


Figure S14. ^{13}C NMR spectrum of $(IT2-S)_2$ (101 MHz, $CDCl_3$).

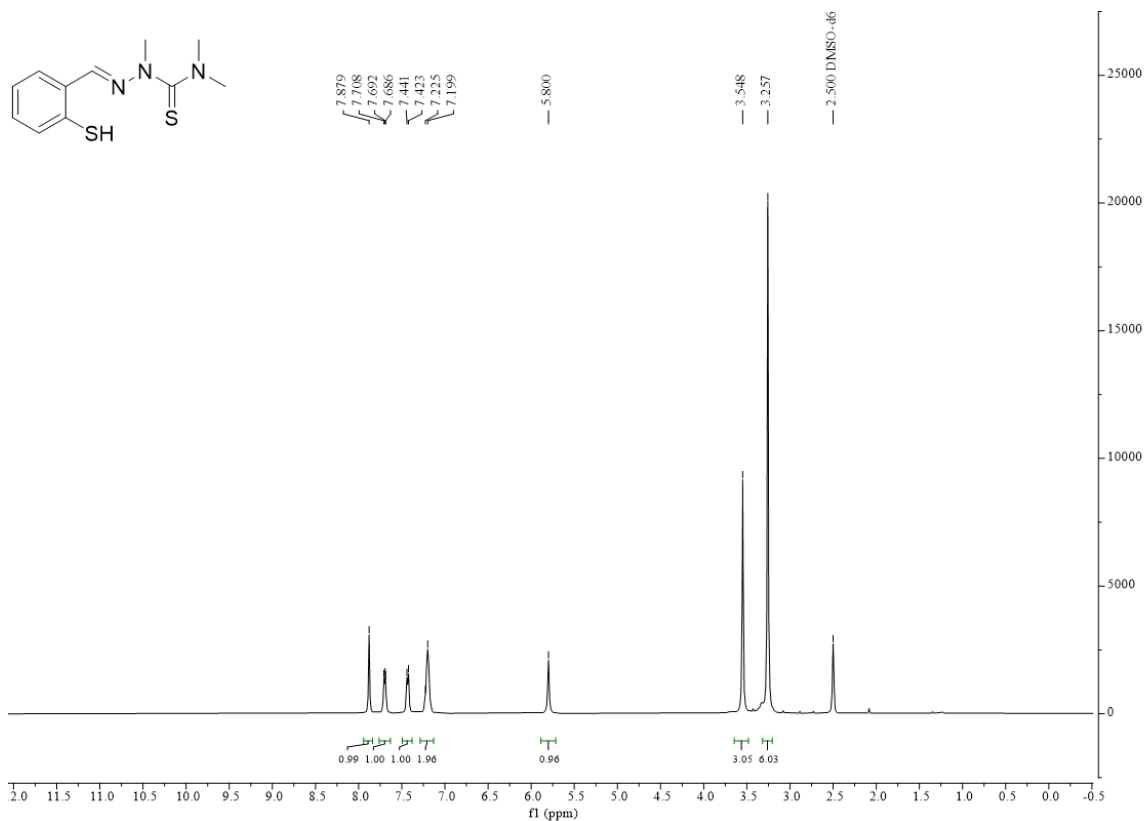


Figure S15. ¹H NMR spectrum of **244mTC** (400 MHz, DMSO-d₆).

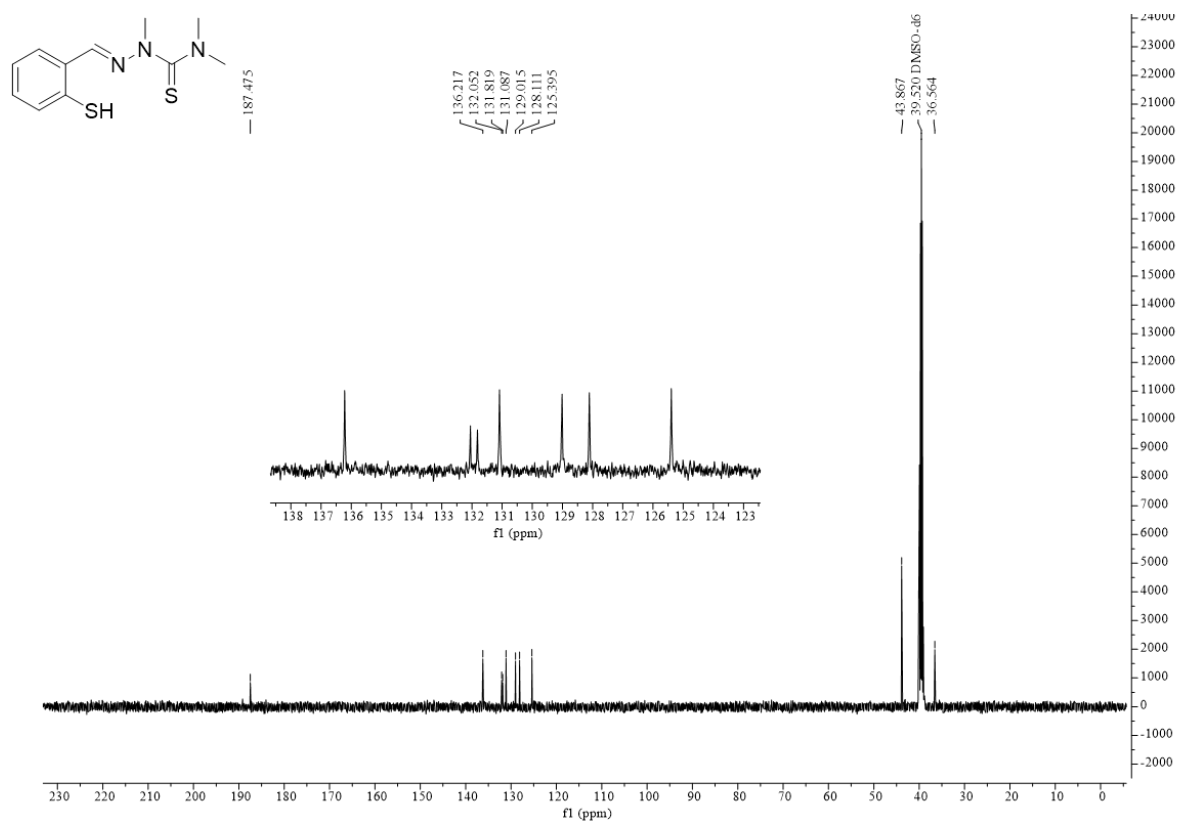


Figure S16. ¹³C NMR spectrum of **244mTC** (101 MHz, DMSO-d₆).

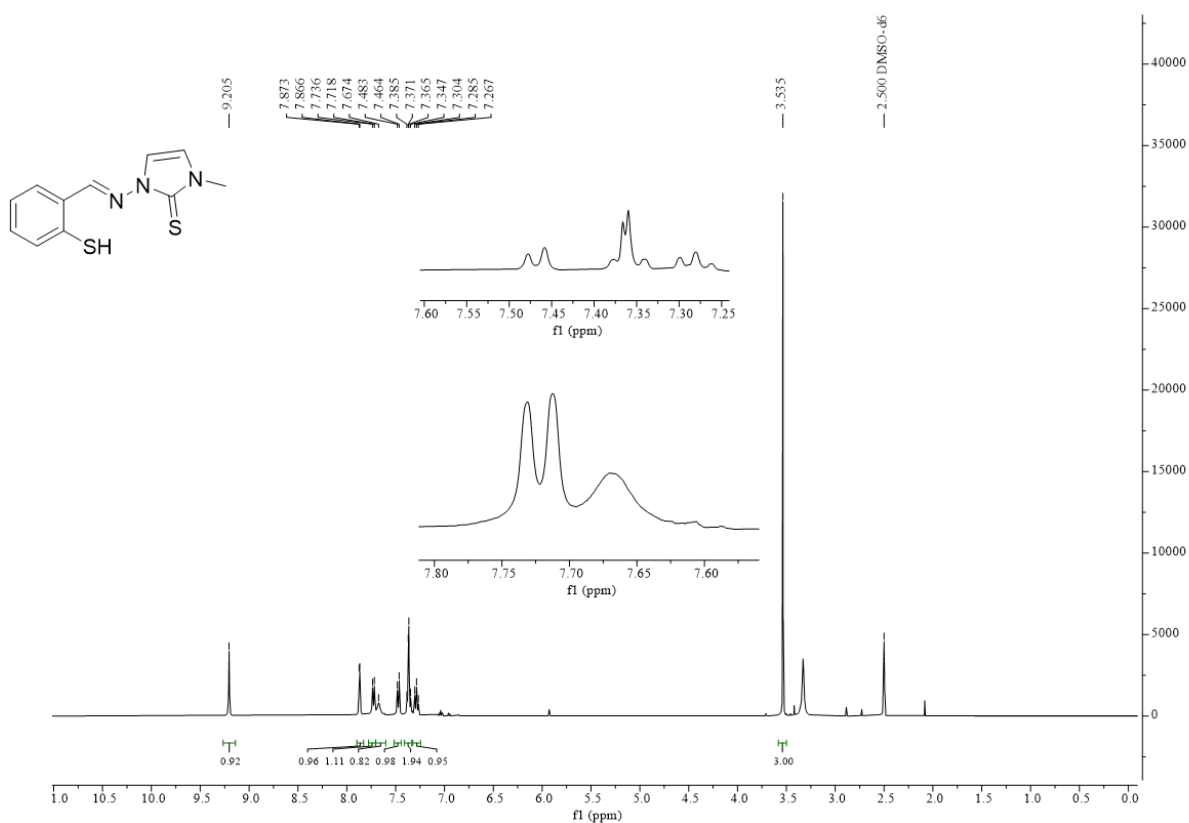


Figure S17. ¹H NMR spectrum of IT1 (400 MHz, DMSO-*d*₆).

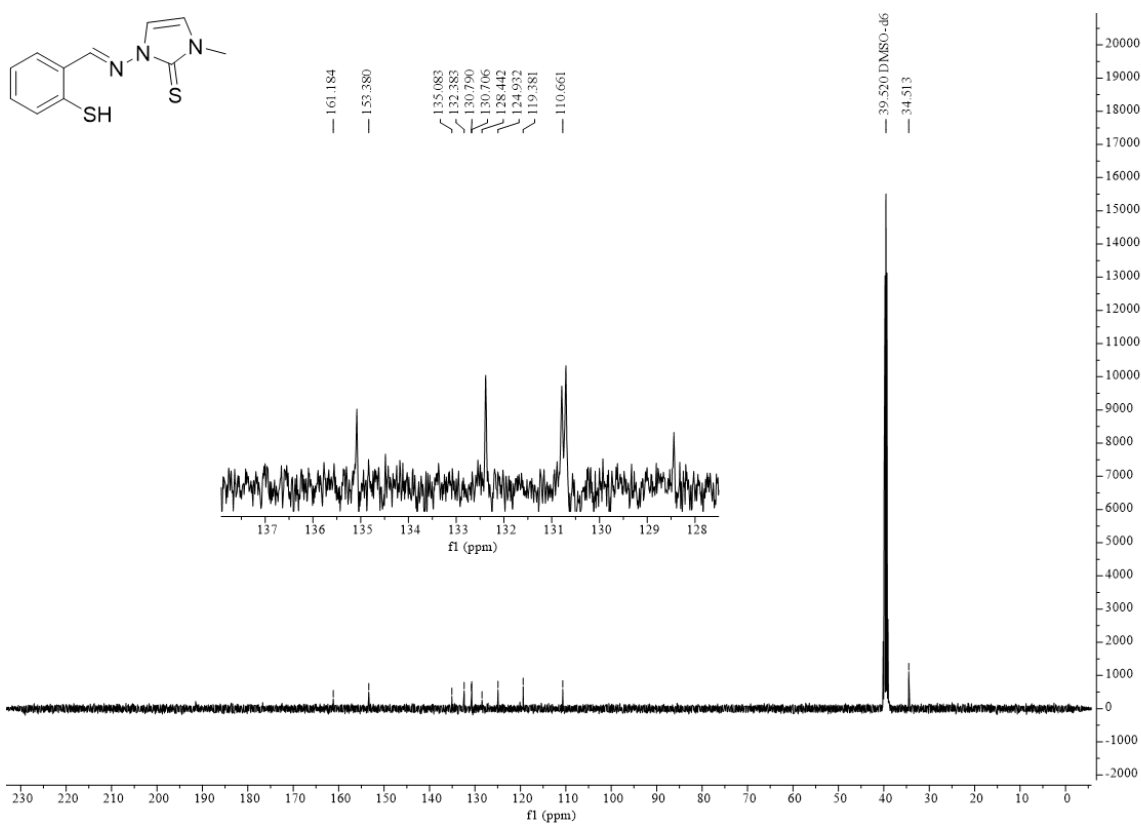


Figure S18. ¹³C NMR spectrum of IT1 (101 MHz, DMSO-*d*₆).